



EE568- Project 4
Hakan Polat
2031243

Contents

1	Introduction	3
2	Literature Review	3
2.1	Torque Output	3
2.2	Manufacturing	3
2.3	Cost	3
2.4	Reliability	4
3	Analytical Modeling of IPM Machine	4
4	FEA Analysis	8
5	Conclusion	12

1 Introduction

In this report, a 6 pole 54 slot I shaped IPM machine is designed for 1.3 MW traction motor. The motor is force air cooled. In the first section, a brief literature review is made to select the suitable motor topology. Then the choosen machine is desined analytically. After the analytical design, the same machine is analyzed using FEA in ANSYS Maxwell environment where the analytical design is validated and the differences are investigated. Finally, the designed machine is compared to other similar machines in the literature and the advantages and disadvantages are discussed.

2 Literature Review

In this section a literature review about the topic of traction motor/generator will be made. During this review, five different subjects will be under investigation namely: Torque output, manufacturing, cost and reliability. According to the initial literature review most common motor topologies employed in traction are induction machine (IM), interior permanent magnet(IPM) machines, surface mount permanent magnet synchronous machine (SM-PMSM) and switch reluctance machine (SRM).

2.1 Torque Output

According to Pellegrino et. al [1]-[2], IPM machines have the highest torque output. Comparted to SM-PMSM and SRM having both the electrical torque and reluctance torque(meaning $L_q \neq L_d$) results in a higher torque output. However, compared to the SM-PMSM the cogging torque is usually higher (depends on the slot number and saliency). Compared to the IM the torque is still higher due to thermal effects. Due to the fact that there is extra winding on the rotor side in an IM, the electrical and magnetic loading of IM's are usually lower than an IPM machine. Having multi rotor interior magnet slot increases the saliency in an IPM machine hence using field weakening methods, IPM machines are also more suitable for over-loading[3]. Moreover, IPM due to high torque output, the power density of this type of EM is usually higher than other topologies.

2.2 Manufacturing

In the perspective of manufacturing, SRM machines are superior not only compared to IM, IPM and SM-PMSM but also other motor topologies which are not under investigation. Since the rotor consists of only single piece (of course laminated) of iron, it is very easy to manufacture it as sheets and combine them. IPM machines are the most problematic due to the need of internal slot for the rare-earth magnets. Moreover, most IPM are not single slotted and hence more magnet slot is usually required.

2.3 Cost

Due to usage of rare eath materials, the cost of machines consisting of permanent magnets are highly dependent on the magnet prices. This is main reason why companies such as BMW and Tesla are converting to IM in their new EV drive train designs [2]. However, again due to ease of manufacturing and lack of rotor magnet and winding , SRM machines are highly superior to other machine types. Then IM are the second best option. Then comes SM-PMSM due to having a relatively easier rotor to manufacture compared to IPM. IPM is the most expensive choise of topology due to the fact that it is more costly to manufacture the rotor structure and also it uses rare earth materials. However, a possible solution is having high saliency in the rotor structure and replace the rare earth material magnets with a ferrite magnet. Although, this reduces the overall power output of the machine in some cases it may be cheaper than SM-PMSM.

2.4 Reliability

Reliability is highly dependent on the operation condition of the machine. SRM is the most reliable machine since it consists of iron rotor structure with no winding or magnet. Therefore, the maximum operation temperatures of SRM machines are higher than other machine types. (assuming same cooling conditions.) Moreover, de-magnetization is an important topic in machines consisting magnets. At high current conditions the magnets in an IPM and SM-PMSM machines can be demagnetized slightly and reduces the power rating of the machine.

3 Analytical Modeling of IPM Machine

The aim of this study is to design a 1.3 MW traction motor. The initial specs of the machine is given in Table 3.

Table 1: Initial Design Parameters

Machine Output Power	1280 kW
Rated Speed	1500 rpm
Rated Voltage	1350 V_{l-l}
Number of Poles	6
Cooling Type	Forced Air Cooled

Since this machine is a traction motor having more than 1 MW of output power, this machine is most probably used in a heavy duty load carrier truck. Since the power output of fully electric EV are around 100-150 kW. Let us start the analysis by selecting a proper machine constant(C_{mech}), a specific magnetic loading (\hat{B}) and specific electrical loading (\hat{A}). C_{mech} is selected from Figure 2 as $270 \text{ kW}/\text{sm}^3$. Which is right in the middle of the curve at $215 \text{ kW}/\text{pole}$

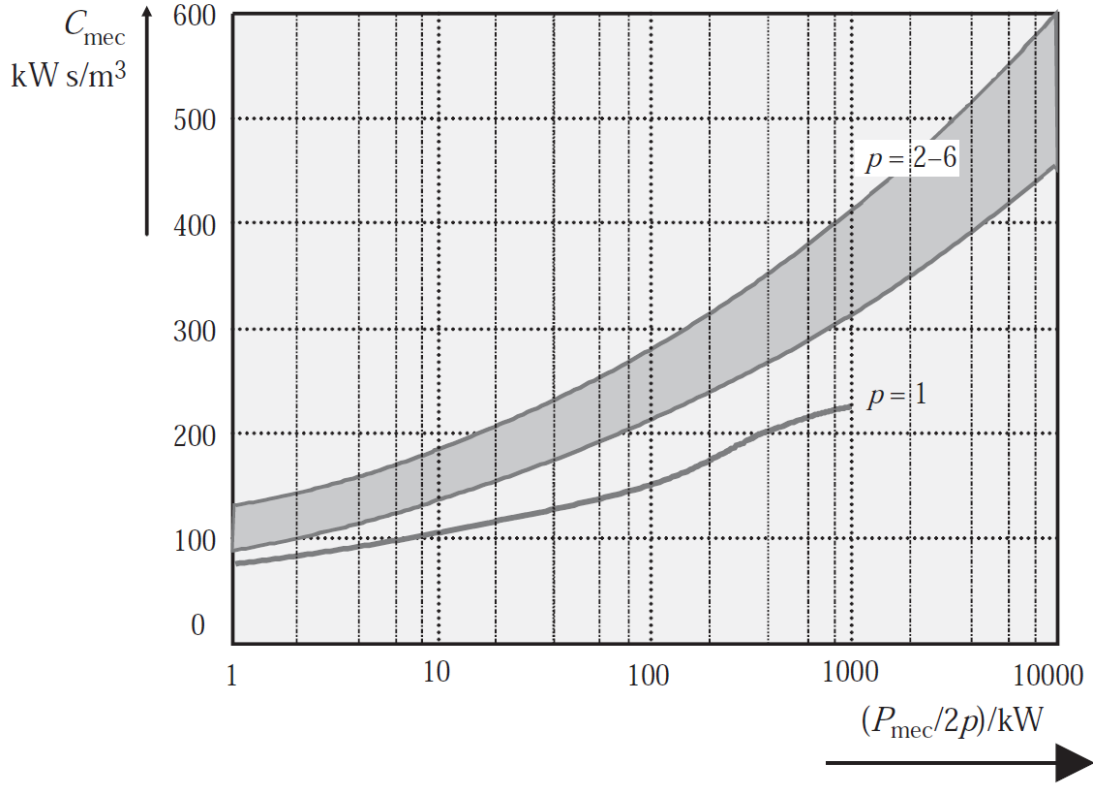


Figure 1: Machine constant-power per pole curve

Specific magnetic loading is given in Eq. 1 and was selected as 0.8 T as initial value. This selection was performed using the rule of thumbs given in the lecture slides. These values also be found in Pyronen.

$$\hat{B} = \frac{p\Phi_p}{\pi D_i L} = 0.8 \text{ T} \quad (1)$$

Therefore the specific electrical loading is found as 71.91 from the Eq. 2. k_w is taken as 0.933.

$$C_{mech} = \frac{\pi^2}{2} k_w \hat{A} \hat{B} \quad (2)$$

The next topic is to determine the rotor diameter. Using typical aspect ratio in Eq. 3, the rotor diameter can be found in Eq. 4.

$$X = \frac{\pi}{4p} \sqrt{p} = \frac{L'}{D_i} = 0.4534 \quad (3)$$

$$D_i = \sqrt[3]{\frac{P_{mech}}{X C_{mech} f}} = 490 \text{ mm} \quad (4)$$

The frequency is found to be 75 Hz, since we have 6 poles and 1500 rpm.

Hence the axial length L' can be calculated as 222 mm.

Next, is the calculation of airgap. The airgap calculation can be found in Eq. 5. The multiplication of 1.6 is due to the fact that the machine is a heavy duty machine.

$$l_{airgap} = 1.6(0.18 + 0.006P^{0.4}) = 1.6(0.18 + 0.006 \times 1300000^{0.4}) = 2.966 \text{ mm} \quad (5)$$

The next subject, is selection of number of stator slots. According to, emeter winding calculator, 6 pole-54 slot with a double layer configuration has a $k_w = 0.945$ and the 3rd and 5th harmonics are nearly eliminated. Although, the reasoning for selection of number of stator slot is missing at this point, actually it was selected iteratively. The stator slot number selection will make more sense as the analytical design continues. In Table 1, the rated voltage is given as $1350V_{l-l}$. A Δ configuration is used. Therefore, the number of turns per phase can be calculated as in Eq. 6.

$$V_{emf} = 1350V = 4.44fk_w N_{ph} \Phi_p \quad (6)$$

From Eq. 6, the number of turns per phase (N_{ph}) is calculated as 72 turns resulting in 8 turns per slot. At this point we are ready to determine the slot dimensions and back core thickness. Since the airgap is known the slot inner diameter (D_{si}) is 496 mm. This machine is for a heavy duty truck and hence easy repair and manufacturing is key. Therefore, parallel slot is chosen resulting in a slot ratio $d = 0.5$. The outer diameter of the slot (D_{so}) is calculated as in Eq. 7.

$$D_{so} = \frac{0.490 \text{ mm}}{0.5} = 980 \text{ mm} \quad (7)$$

Hence, the slot height can be calculated as in Eq. 8.

$$h_{slot} = \frac{D_{so} - D_{si}}{2} = 248 \text{ mm} \quad (8)$$

Now, let us find the slot thickness. Initially, take assume half of the circumference is the slot. Hence average width of trapezoidal slot can be found as in Eq. 9.

$$w_{slot,avg} = \frac{\pi(D_{si} + D_{so})}{2} \frac{1}{2 \times 54} = 14 \text{ mm} \quad (9)$$

Hence, the slot area can be calculated as in Eq. 10.

$$A_{slot} = w_{slot,avg} h_{slot} = 14 \times 248 = 3742 \text{ mm}^2 \quad (10)$$

The next arising question is that whether we can fit the coils in the slot. To calculate we need to choose a AWG wire.

The phase current can be found from Eq. 11.

$$P_{mech} = 3V_{phase} I_{phase} \quad (11)$$

From Eq. 11 I_{phase} can be found as 555A. By choosing a current density $J = 4A/mm^2$, the required coil area can be found as 111 mm^2 . Therefore, 2 parallel strands of AWG0(53 mm^2) can carry the necessary current. Moreover, assuming a fill factor of 0.4, the slot area is bigger than the copper area. The calculation is given in Eq. 12.

$$A_{copper} = 8 \times 111 = 888 \text{ mm}^2 < A_{slot} \times k_{fill} = 1388 \text{ mm}^2 \quad (12)$$

Therefore, the coppers can fit into the slot. We can also decrease the slot width further more in order to enhance the both the heat conduction and reduce the teeth magnetic field density. A down-side is the increases iron mass.

The final geometric unknown parameter is the back-core thickness. The back core thickness is calculated such that the maximum B is 1 T. The back-core thickness calculation can be found in Eq. 13 where $k_{stacking}$ is taken as 0.95 and the back-core thickness is denoted as h_{ys} .

$$B = \frac{\Phi_{pole}}{2k_{stacking} L' h_{ys}} = 1 \text{ T} \quad (13)$$

Using Eq. 12, h_{ys} can be found as 10 cm.

Re-calculation of the specific electrical loading is given in Eq.13 .

$$\hat{A} = \frac{N_{slot} Q I}{\pi D_i} = \frac{8 \times 54 \times 555}{\pi \times 0.490} = 155 \text{ kA} \quad (14)$$

At this stage all required geometric parameters are known. The initial results are listed in Table 2.

Table 2: EML System Constants

D_{rotor}	490 mm
Air gap	2.96 mm
D_{si}	496 mm
D_{so}	980 mm
h_{slot}	248 mm
w_{slot}	14 mm
h_{ys}	100 mm
N_{ph}	54 turns
N_{slot}	8 turns
Number of Pole	6
Number of Stator Slot	54
Layer configuration	Double Layer
Coil Span	8 slots

The winding diagram of the proposed machine is presented in Fig. 2.

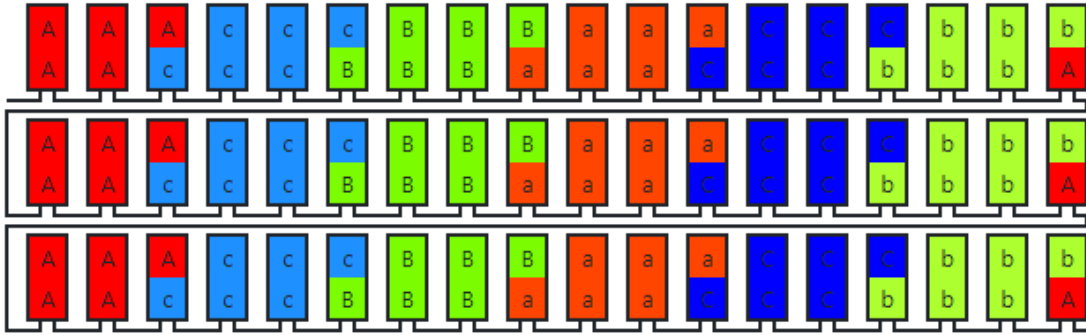


Figure 2: Winding diagram of the proposed 6pole-54slot machine.

Until this point, we assumed linear material properties. We assumed infinite permeability of the iron core. However, in practice selection of core material, lamination and the magnet material has a huge impact on both loss estimation and overall machine cost. Initially, the specific magnetic loading was selected as 0.8T. Specific magnetic loading was given in Eq. 1. We know that the airgap is 3 mm. In an IPM machine the magnets are buried inside the rotor core. Hence we need to determine the magnet height. We can assume pole to magnet ratio as 0.8 which is a reasonable selection.

The calculation is as follows.

$$R_g = \frac{l_g}{\mu_0 A} = \frac{3mm}{\mu_0 \pi 0.8 D_i L} = 27433 H^{-1} \quad (15)$$

Now assume 10 mm magnet height. (Note that it is just and initial guess.)

$$R_m = \frac{l_m}{\mu_0 A_m} = \frac{l_m}{\mu_0 \pi 0.8 D_i L} = \frac{l_m}{9.14e^6} = 9.14e^4 H^{-1} \quad (16)$$

Assume N42H magnet.

$$F = B_r A_m R_m = 1.33 * 0.2734 * 91400 = 33235 NI \quad (17)$$

Since we selected slot to pole ratio as 0.8 we need an $B_{op} = 1T$.

$$B_m = \frac{F}{A_m(R_g + R_m)} = 1.02T \quad (18)$$

Here it is important to note that initial selection of 10 mm of magnet height was at random. If B_m was found lower than 1T, a reduction of magnet height was necessary and visa versa.

Now let us select a core material. In order to make it cheap ChinaSteel-35CS440 is selected for both rotor and stator iron material.

4 FEA Analysis

First the model was built using RMXprt then was exported to Maxwell 2D. Since we have 54 slot and 6 pole we can use 1/6 symetry during analysis. The FEA model is presented in Fig. 3.

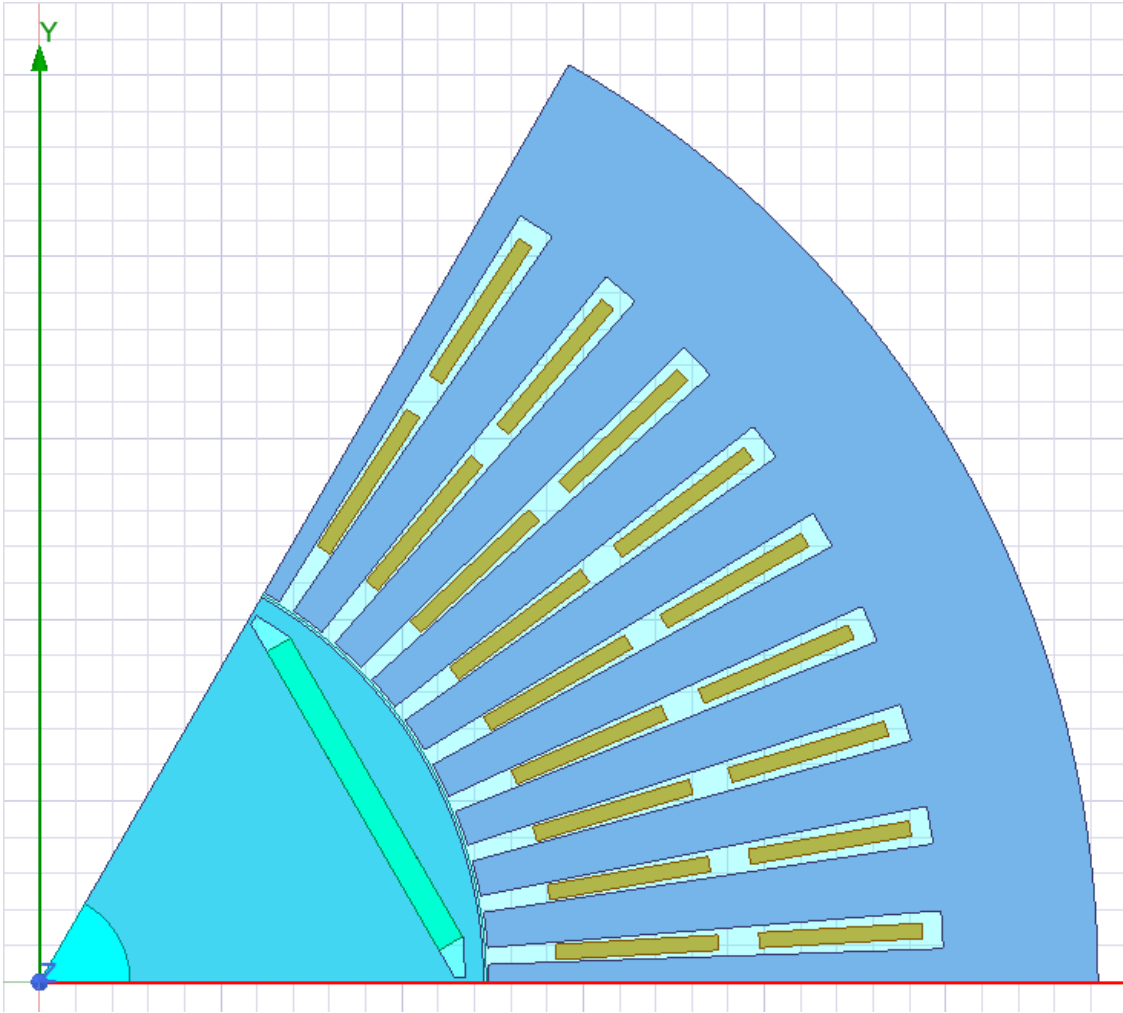


Figure 3: 1/6 symmetric model of the designed IPM machine

In RMXprt the cogging torque is found and presented in Fig. 4.

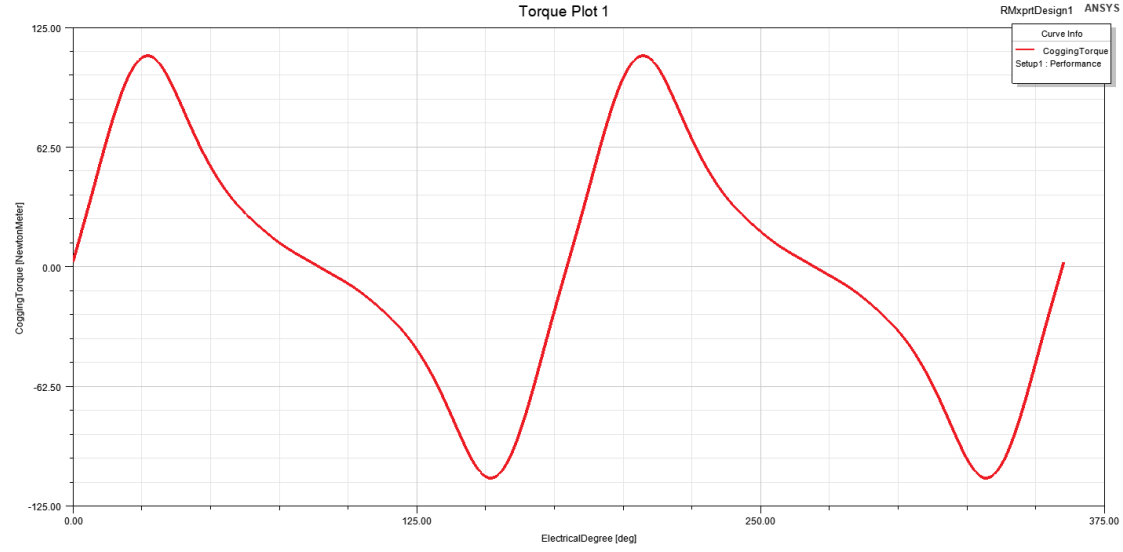


Figure 4: Cogging torque of the designed machine

According to the results in Fig. 4, the cogging torque oscillates between ± 112 Nm. The airgap flux density is presented in Fig. 5.

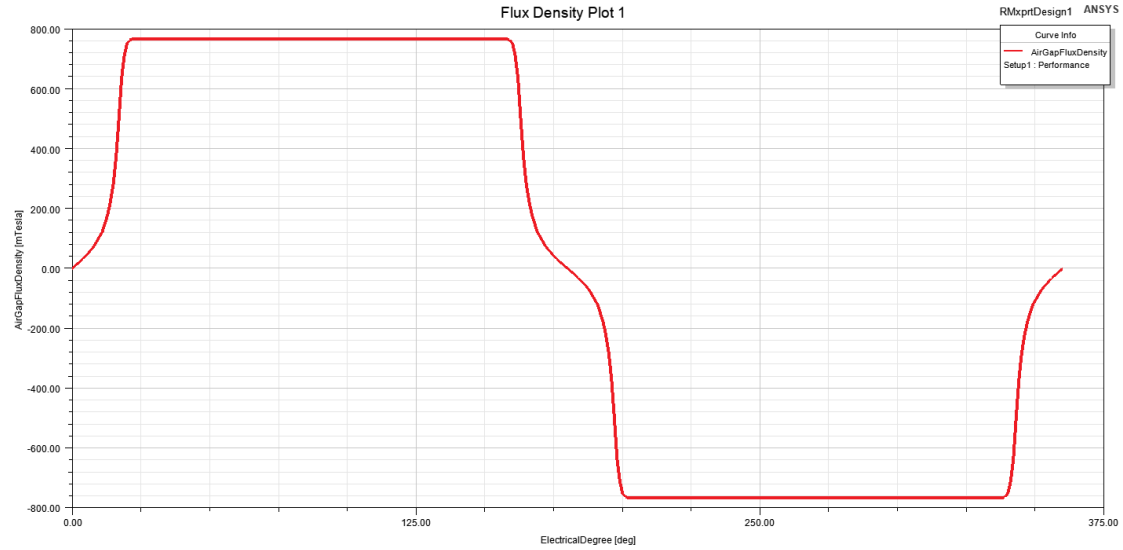


Figure 5: Airgap flux density

The maximum value is very close to the analytical design. The slight deviation is due to ignoring rotor and stator reluctances. Moreover, since the magnets are buried inside of the machine, there is also a slight leakage inductance. The air-gap at the ends of the magnets is used to reduce the leakage inductance. A magnetostatic analysis is used to calculate the L_d and L_q . Since an IPM machine has saliency, the results should be different. The L_q is found to be 20.5 mH while L_d is found to be 9.5 mH. Moreover, using the same FEA model the phase inductance is found to be 6.96 mH. The induced voltage is found with a transient analysis where the current input to the stator coils are set to be 0 amperes. The induced voltage waveforms are presented in Fig. 6. In the model the rotational speed is

set to be 1500rpm.

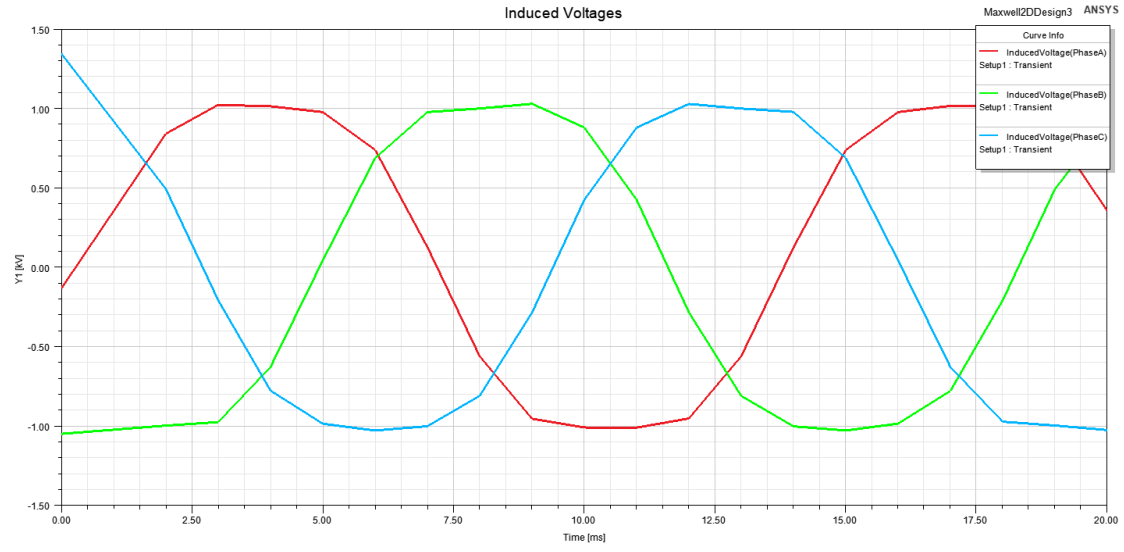


Figure 6: Induced voltages.

The induced voltage have a sinusoidal waveform with a few harmonics. The rms value of the fundamental component is $720V_{rms}$. Here it is important to note that the connection was Wye connection hence the line-to-line voltage (V_{l-l}) is 1247 V which is close to the initial design value.

Finally, let us investigate the B field distribution during rotation. The B field distribution is presented in Fig. 7.

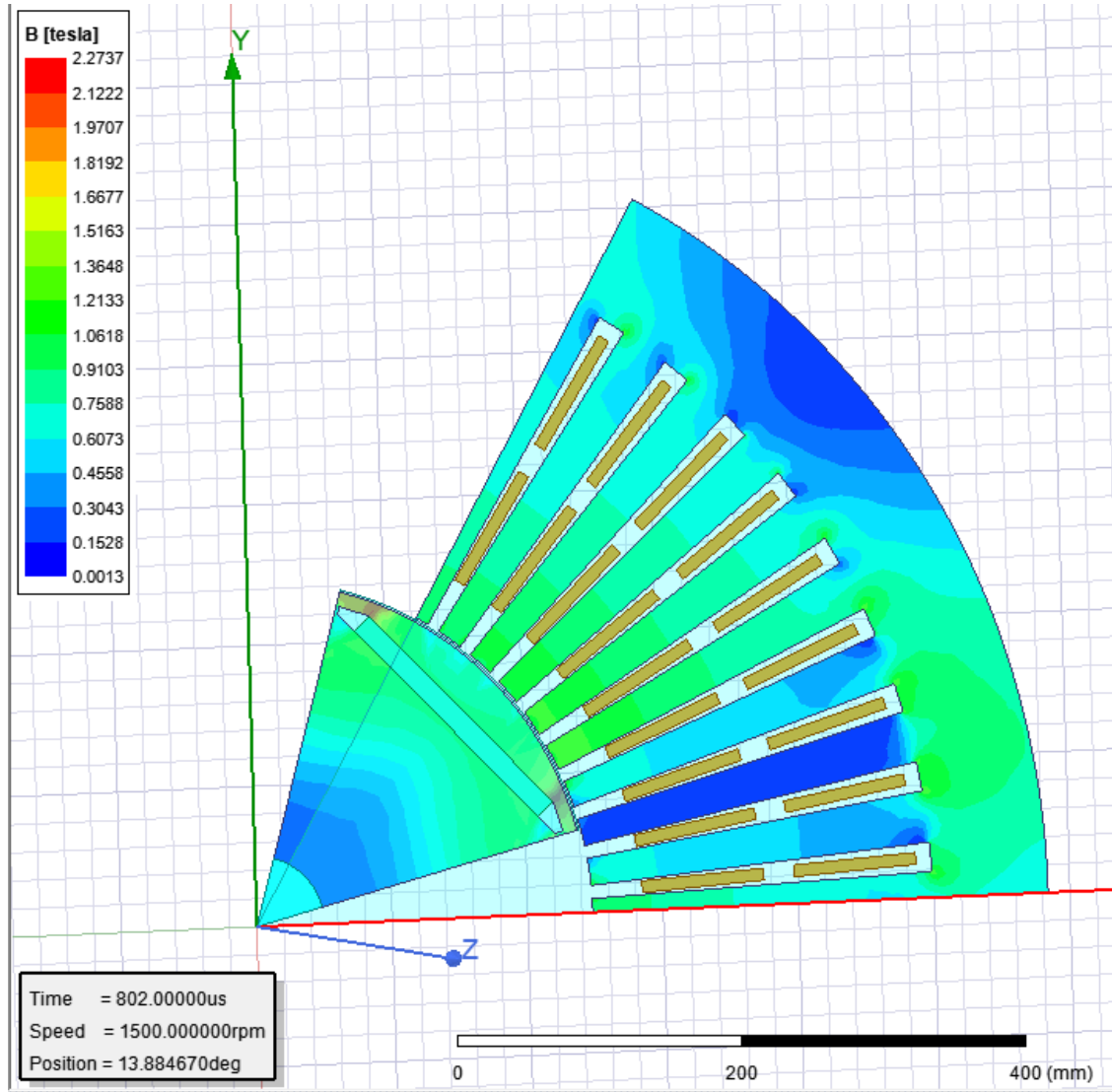


Figure 7: Induced voltages.

According to Fig. 7, the airgap-B is around 0.8 which was previously found. Moreover, the maximum teeth B field magnitude is around 1.25T which is within the design limitations. The back-core has a maximum of 1.07 T which was again our design criteria.

5 Conclusion

In this report a 6 pole 54 slot IPM machine was designed both analytically and using FEA model. The end results are very close to each other. The main parameters of the designed machine is given in Table 3.

Table 3: EML System Constants

D_{outer}	1180 mm
l	222 mm
X	0.4534
Torque Density	3353 Nm/m^3
Power Density	1585 W/m^3
Stator Mass	1233 kg
Rotor Mass	263 kg
Magnet Mass	455 kg
Copper Mass	95 kg(including the end winding.)

Now, let us compare the designed machine with other machines which are commonly found in the literature. Although a few stator designs are presented in the literature, its design is highly related to its power levels. In the literature, most common IPM examples are found for EV, which have a rated power around 100-150 kW. Since the current levels are low compared to our designed 1.3MW machine, the cable sizing of such motors are smaller. Therefore, needle winding is usually employed where the coils are inserted using a winding machine (Toyota Prius). This reduces the cogging torque and leakage inductance significantly however, as the power levels increase pre made coils are necessary. The cable cross-section of our machine is found to be 100 mm^2 which is hard to work with.

However, there are quite a lot of rotor designs hence the ups and downs of our machine compared to other rotor structures will be discussed. Consider the rotor structures given in Fig.8.

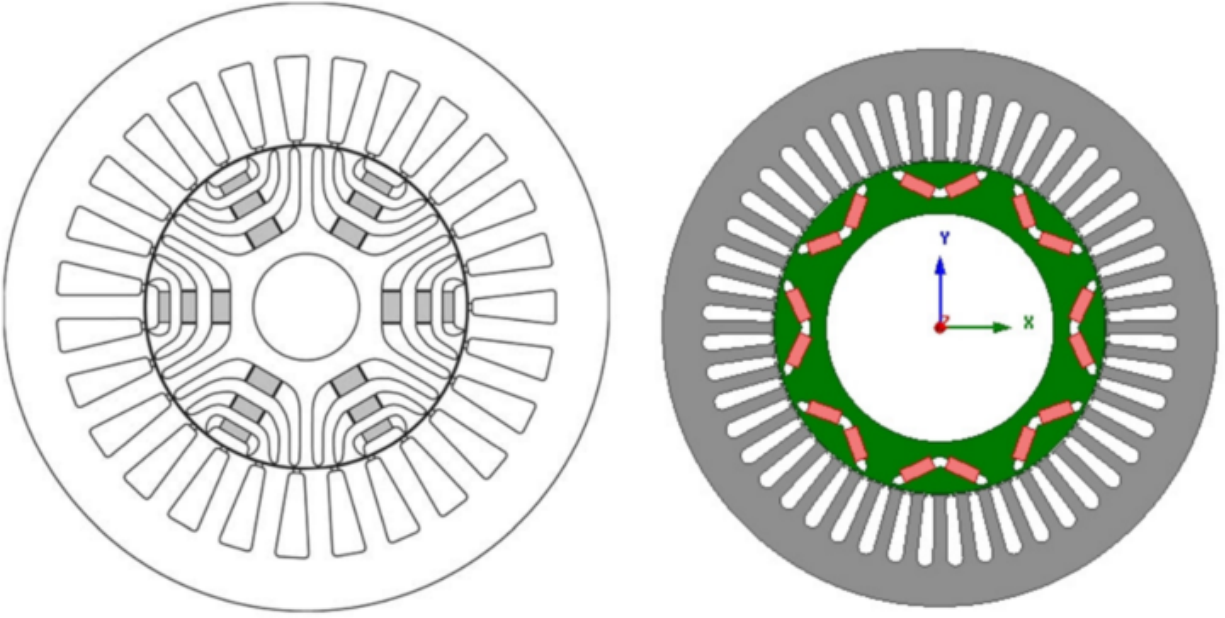


Figure 8: Different rotor geometries

The first rotor in Fig 8, has 3 buried magnets for a 6 pole machine. Due to high number of slots in the stator, the saliency of this kind of machines are high. Therefore, the torque output of this kind of machines are higher at lower speeds. This kind of rotor structure is harder to manufacture. Moreover, due to magnet islanding (meaning the flux generated from the magnets flows from the slots) rotor losses increases. Since these machines have already high torque, the magnets can be replaced with ferrite magnets to reduce the cost.

The second rotor structure is from the Toyota Prius 2004. The difference in this machine is the non radial magnets. It is called the V shape. In the literature, having this structure can reduce the magnet mass and hence the cost of the overall machine. However, in terms of back-emf I shaped(our design) rotor design has a much better performance.[4]

I choose the I shaped rotor structure due to its ease of manufacturing and better back-emf performance. However, the designed machine has a lower torque and may have a slightly higher mass of rare-earth magnet. Compared to the first rotor, it is mechanically more stable.

References

- [1] G. Pellegrino, A. Vagati, B. Boazzo, and P. Guglielmi, "Comparison of induction and PM synchronous motor drives for EV application including design examples," *IEEE Transactions on Industry Applications*, vol. 48, no. 6, pp. 2322–2332, 2012.
- [2] J. De Santiago, H. Bernhoff, B. Ekerghård, S. Eriksson, S. Ferhatovic, R. Waters, and M. Leijon, "Electrical motor drivelines in commercial all-electric vehicles: A review," *IEEE Transactions on Vehicular Technology*, vol. 61, no. 2, pp. 475–484, 2012.

- [3] G. Pellegrino, A. Vagati, P. Guglielmi, and B. Boazzo, "Performance comparison between surface-mounted and interior PM motor drives for electric vehicle application," *IEEE Transactions on Industrial Electronics*, vol. 59, no. 2, pp. 803–811, 2012.
- [4] R. Liu, X. Sun, J. Gong, and S. Guo, "Comparison of different arrangement of magnets for the purpose of reducing magnet usage in designing an IPM motor for Electric Vehicles," *IEEE Transportation Electrification Conference and Expo, ITEC Asia-Pacific 2014 - Conference Proceedings*, pp. 1–5, 2014.